Available online at www.sciencedirect.com
ScienceDirect
International Journal of Machine Tools & Manufacture 48 (2008) 677–687
INTERNATIONAL JOURNAL OF MACHINE TOOLS & MANUFACTURE DESIGN, RESEARCH AND APPLICATION
www.elsevier.com/locate/ijmactool

A 3-D modular fixture with enhanced localization accuracy and immobilization capability

Yu Zheng*, Wen-Han Qian

Robotics Institute, Shanghai Jiao Tong University, Shanghai 200240, PR China

Received 18 July 2007; received in revised form 19 October 2007; accepted 29 October 2007
Available online 13 November 2007

Abstract

Modular fixtures are distinguished for their high flexibility. Previous researches focused on 2-D objects or 3-D objects with regular geometry. This paper introduces our systematic study of 3-D modular fixtures, particularly for complex objects. For the sake of both function and simplicity, three baseplates are arranged equilaterally. One baseplate is fixed horizontally, on which three fixels are installed to support the object. The other baseplates are moveable and at least one fixel is set on either of them. Totally, seven fixels are adopted. Efficient algorithms are presented for computing optimal fixel locations for the given object pose regarding localization accuracy and immobilization capability. On account of the manufacturing errors, measuring and adjusting techniques are developed to improve the localization accuracy. Case studies are investigated to illustrate applications. Experiments are performed for verifying the principles, including the well-known theoretical proposition that seven fixels are necessary and sufficient for fixturing a 3-D object of nonrevolutionary surface.

Keywords: Modular fixture; Fixture planning; Localization accuracy; Immobility; Form-closure

1. Introduction

Fixtures are used to hold objects in many manufacturing processes, such as machining, assembly, and inspection. They must satisfy two requirements [1]:

(1) *Localization*: Once touching the locators, the object has a unique position and orientation. This means that the object cannot move without separating from the locators.
(2) *Immobilization*: Once being located and clamped, the object is completely restrained and cannot separate from the fixturing elements (fixels) including locators and clamps. This property is also termed form-closure. By the duality between motions and wrenches, this implies that any external wrenches on the object can be equilibrated.

As the objects in modern manufacturing are increasingly diverse, fixtures are desired to be reconfigurable, immediate, simple, and cheap (RISC). To date, the most popular RISC fixturing system is the modular fixture [1–13], which typically comprises a set of standard elements, including baseplates, locators, and clamps. On the baseplate, there is a lattice of precisely spaced holes. The locators are precisely manufactured, which may be inserted in the holes to locate an object. For fixturing different objects, one needs only to alter the choice of holes for the locators and adjust the clamp(s). In reconfiguration, most elements can be utilized repeatedly.

To facilitate the use of modular fixtures, a series of automated algorithms for computing fixel locations were advanced. Brost and Goldberg [2] gave a complete algorithm for synthesizing modular fixtures for polygonal parts with three round locators and one translating clamp. Wallack and Canny [3] put forward an algorithm for planning modular and hybrid fixtures for generalized polygons with two jaws, each having two round locators. Wallack [4] also discussed other types of modular fixtures and proposed a generic fixture design algorithm. Wu et al. [5,6] expanded Brost–Goldberg algorithm to 3-D objects

*Corresponding author. Tel.: +86 21 54520419.
E-mail address: yuzheng001@gmail.com (Y. Zheng).

0890-6955/$ - see front matter © 2007 Elsevier Ltd. All rights reserved.
doi:10.1016/j.ijmachtools.2007.10.022

with horizontal or vertical planar or cylindrical surfaces. They also considered the locators having various shapes and other quality criteria, such as accuracy, clamping, and accessibility. Pham and Lazaro [7], Dai et al. [8], Kumar et al. [9,10], and Hou and Trappey [11] brought forth the CAD-based methods for automated fixture design. Qian and Qiao [12] offered an efficient algorithm for computing the object poses matching the given fixel locations. Mervyn et al. [13] brought forward an evolutionary search algorithm for exploring the possible fixture designs and suggesting an appropriate one. Some work [14,15], although not directly related, may also contribute to the research on modular fixtures. In addition, since modular fixtures and modular grippers have many similarities, their researches could benefit from each other [16,17].

Some previous work on modular fixtures considers just 2-D objects [2,3,12]. They can only be applied to cylindrical objects with small height. Many efforts have been made for fixturing 3-D objects, but the object surfaces are piecewise planar or cylindrical [5–11,16]. Wang and Pelinescu [14] and Wang et al. [15] presented two new methods of optimizing fixture layout for complex objects, which are not specifically dedicated to modular fixtures.

In this paper, we first elaborate a prototype of 3-D modular fixture. Different from Wallack's tetrahedral arrangement of four baseplates [4], we arrange three baseplates equilaterally, on which seven fixels are allocated. An algorithm is developed for finding all feasible fixel locations on each baseplate. Then by the criteria of localization [14] and immobilization [18], we provide algorithms for picking out the fixel locations such that both localization accuracy and immobilization capability of the configured fixture are optimal. Since the manufacturing errors of the fixture are inevitable, we try to compensate for them by measuring the gripped object and adjusting the lengths of fixels. Proved to be very effective by experiments, this technique can be used readily in production.

2. A rational 3-D modular fixture

2.1. Setup

Noting that six points are sufficient for locating 3-D objects without rotational symmetry and seven for immobilizing, we use totally seven fixels for fixturing an object. The fixels are cylindrical and each makes a point contact with the object by its spherical end. We require the fixels to contact the object in different directions so that form-closure can be achieved easier. On two antipodal baseplates (Fig. 1(a)), the fixels approach an object in opposite directions. Thus, some areas of the object surface become very bad for fixels to contact: the fixel is too long and its inclination angle w.r.t. the surface normal is too large. On four tetrahedral baseplates (Fig. 1(b)), the fixels can reach wider object surface, but the open space for tools to access is narrower and the structure is complicated. For a tradeoff, we place three baseplates equilaterally around an axis of symmetry. The seven fixels are allocated on the baseplates. Each baseplate has at least one.

If the baseplates together with their axis of symmetry are placed vertically, their functions in fixturing are identical. However, how to load the object firmly before clamping is problematic. Hence, we let the axis be horizontal and put a horizontal baseplate below, just as shown in Fig. 1(c). To simplify the structure but retain the flexibility of the fixture, the bottom baseplate is fixed, while the upper two can move towards the aforementioned axis (Fig. 2). Three fixels are settled on the bottom baseplate so that the object can rest stably on them at the beginning of fixturing process. The other four fixels have two arrangements on the upper two baseplates, i.e., two on each or three on the left and one on the right, which are analogous to the $\{2+2\}$ and $\{3+1\}$ arrangements of four fixels on the 2-D modular fixtures [2,3]. Thus, seven fixels have two normal arrangements on the baseplates, denoted by $\{3+2+2\}$ and $\{3+3+1\}$, where the three numbers in turn represent the numbers of fixels located on the bottom, left, and right baseplates. The former two refer to locators, while the last

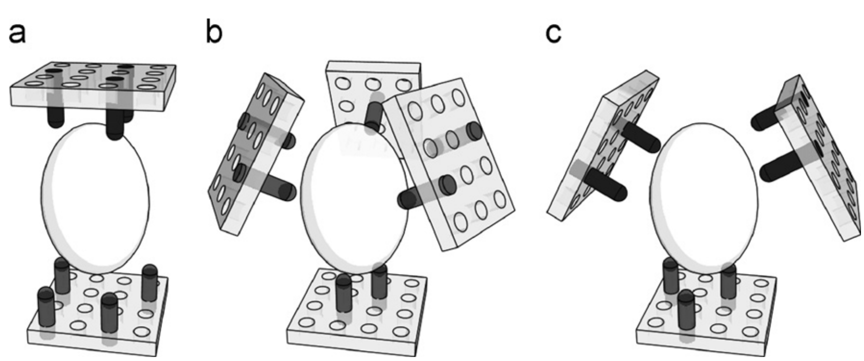

Fig. 1. Comparison of different baseplate placements: (a) Two antipodal baseplates. The fixturing structure is simple but the object surface within touch of fixels is limited. (b) Four tetrahedral baseplates. A wider object surface can be touched but the fixturing structure is more complex. (c) Three equilateral baseplates embody a rational compromise. Three fixels on the bottom plates can stably support the object before clamping.

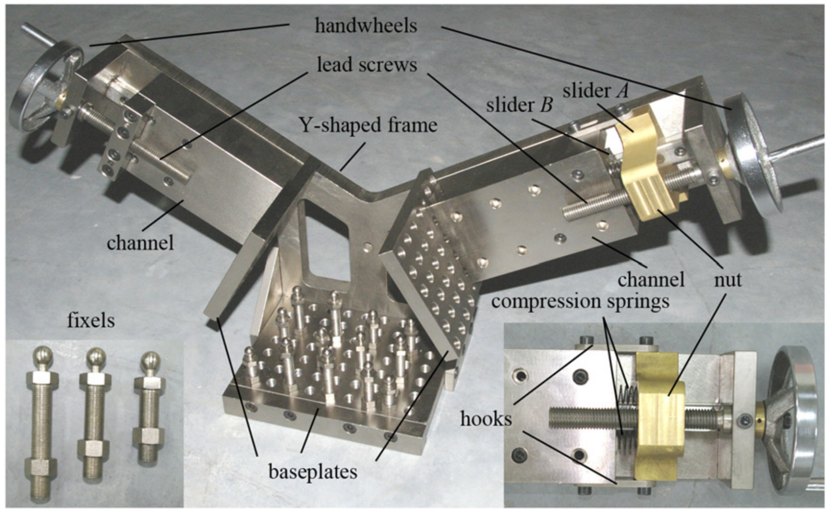

Fig. 2. Prototype of the modular fixture.

number has clamping function or is a clamp indeed. Accordingly, the right baseplate is flexible.

To carry out this idea, we first set up a Y-shaped vertical plate as the frame for assembling the baseplates, as shown in Fig. 2. Using one Y-shaped plate rather than two parallel is to open larger space for the access of tools. The horizontal baseplate is attached to the bottom of the frame. On either arm we install a guide, and a baseplate is connected to the slider on the guide through a channel, which covers the slider. We do not use a strip of steel but a channel as the connector between the slider and the baseplate in order to strengthen the joints and position the baseplate w.r.t. the slider better. Such guides and sliders in pairs are commercially available, e.g., THK and NSK brands. Since the left and right fixels have different functions in locating and clamping, the configurations of the driving mechanisms are somewhat different, although either slider is driven by a handwheel, whose rotation is transformed by a screw transmission into the translation of a nut along the guide. On the left, the nut is fixed rigidly on the slider. On the right, the nut is made of bronze and enlarged as an additional slider A behind the slider B on the same guide fastened with the baseplate. Two compression springs are installed between sliders A and B and precompressed by two hooks linking A and B (Fig. 2). Driven by the right handwheel, the sub-assembly comprising the nut annexed to slider A, the springs, slider B, the channel, the hooks, the baseplate and the fixels can move along the guide to and fro as a whole. Once the fixel(s) contact(s) the object, further turning the handwheel causes an additional compression of the springs and exerts a clamping force on the object. The setup is reinforced by two triangular stiffeners connecting the bottom baseplate with the vertical frame.

There are 9×7 holes on the bottom baseplate and 6×7 on the others. The fixels are screwed into the lattice holes so that their lengths can be adjusted slightly to compensate for the location error. Also, ready-made fixels of different lengths can be selected (Fig. 2).

2.2. Mathematical model

We first establish a framework for the later computation of fixtures. Let $\mathscr{F}_{\mathrm{B}}$, $\mathscr{F}_{\mathrm{L}}$, and $\mathscr{F}_{\mathrm{R}}$ denote the coordinate frames attached to the bottom, left, and right baseplates, respectively, called the plate frames. Frame $\mathscr{F}_{\mathrm{B}}$ is also used as the fixture frame. The origin of each frame is located at the plate center. Then the positions and orientations of $\mathscr{F}_{\mathrm{L}}$ and $\mathscr{F}_{\mathrm{R}}$ w.r.t. $\mathscr{F}_{\mathrm{B}}$ are

$$\boldsymbol{p}_{\mathrm{B,L}} = \begin{bmatrix} 0 \\ -s_{\mathrm{L}}\cos\varphi \\ H + s_{\mathrm{L}}\sin\varphi \end{bmatrix}, \quad \boldsymbol{R}_{\mathrm{B,L}} = \begin{bmatrix} 1 & 0 & 0 \\ 0 & -\sin\varphi & \cos\varphi \\ 0 & -\cos\varphi & -\sin\varphi \end{bmatrix},$$

$$\boldsymbol{p}_{\mathrm{B,R}} = \begin{bmatrix} 0 \\ s_{\mathrm{R}}\cos\varphi \\ H + s_{\mathrm{R}}\sin\varphi \end{bmatrix}, \quad \boldsymbol{R}_{\mathrm{B,R}} = \begin{bmatrix} 1 & 0 & 0 \\ 0 & -\sin\varphi & -\cos\varphi \\ 0 & \cos\varphi & -\sin\varphi \end{bmatrix},$$

where s_{L} and s_{R} are the translational distances of the left and right baseplates along their sliders, $H = 85\,\mathrm{mm}$ is the height of the foregoing axis, and $\varphi = \pi/6$ is the inclination angle of the sliders. The x and y coordinates of fixel i in the plate frame are $\lambda_{i_1}a_1$ and $\lambda_{i_2}a_2$, where a_1 and a_2 are the spaces of the hole center lattice and both equal to 20 mm; λ_{i_1} can take any integer in $[-3, 3]$ for any fixel, and λ_{i_2} can take any integer in $[-4,4]$ for the fixels on the bottom baseplate and any number in $\{-2.5, -1.5, -0.5, 0.5, 1.5, 2.5\}$ for the others. Let λ_{i_3} be a positive real designating the z coordinate of the spherical end. Then the location of fixel i is denoted by $(\lambda_{i_1}, \lambda_{i_2}, \lambda_{i_3})$, and its end is expressed in the plate frame as the sphere of radius r_i centered at $\boldsymbol{e}_i = [\lambda_{i_1}a_1 \quad \lambda_{i_2}a_2 \quad \lambda_{i_3}]^{\mathrm{T}}$, denoted by F_i. Fixel i in the fixture frame is given by

$$F_{\mathrm{B},i} = \boldsymbol{R}_{\mathrm{B}}(F_i) + \boldsymbol{p}_{\mathrm{B}},$$

where $\boldsymbol{R}_{\mathrm{B}}=\boldsymbol{I}$, $\boldsymbol{R}_{\mathrm{B,L}}$, $\boldsymbol{R}_{\mathrm{B,R}}$ and $\boldsymbol{p}_{\mathrm{B}}=\boldsymbol{0}$, $\boldsymbol{p}_{\mathrm{B,L}}$, $\boldsymbol{p}_{\mathrm{B,R}}$ for fixels on the bottom, left, and right baseplates, respectively.

Denote the object by a compact set O of $\mathbb{R}^3$. Let $\mathscr{F}_{\mathrm{O}}$ denote the object coordinate frame, and $\boldsymbol{p}_{B,O}\in\mathbb{R}^3$ and $\boldsymbol{R}_{B,O}\in SO(3)$ the origin and orientation of $\mathscr{F}_O$ w.r.t. $\mathscr{F}_{\mathrm{B}}$. Then O in $\mathscr{F}_{\mathrm{B}}$ is given by

$$O_{\mathrm{B}}=\boldsymbol{R}_{B,O}(O)+\boldsymbol{p}_{B,O}.$$

The geometrical relationship between a fixel and the object is measured by the distance function $d(F_{\mathrm{B},i}, O_{\mathrm{B}})$ of $F_{\mathrm{B},i}$ and O_{B}. The distance function is introduced in the Appendix. For the cases of separation, contact, and penetration, the value of $d(F_{\mathrm{B},i}, O_{\mathrm{B}})$ is positive, zero, and negative, respectively. If the object O is convex, then from the Appendix $d(F_{\mathrm{B},i}, O_{\mathrm{B}})$ can be computed by

$$d(F_{\mathrm{B},i},O_{\mathrm{B}})=-\min_{\|u\|=1}\Big(\boldsymbol{u}^{\mathrm{T}}(\boldsymbol{R}_{\mathrm{B}}\boldsymbol{e}_i+\boldsymbol{p}_{\mathrm{B}})+r_i - \min_{x\in O}\boldsymbol{u}^{\mathrm{T}}\boldsymbol{R}_{B,O}\boldsymbol{x}-\boldsymbol{u}^{\mathrm{T}}\boldsymbol{p}_{B,O}\Big). \quad (1)$$

When $d(F_{\mathrm{B},i}, O_{\mathrm{B}})=0$, the unit vector $\hat{\boldsymbol{u}}$ for which the above minimum value is attained indicates the normal at contact outward to $F_{\mathrm{B},i}$ and inward to O_{B}, and then the contact point on the object surface in $\mathscr{F}_{\mathrm{B}}$ can be written as

$$\boldsymbol{r}_{\mathrm{B},i}=\boldsymbol{R}_{\mathrm{B}}\boldsymbol{e}_i+\boldsymbol{p}_{\mathrm{B}}+r_i\hat{\boldsymbol{u}}. \quad (2)$$

3. Computing optimal fixel locations

In what follows, we try to compute the fixel locations w.r.t. the given $\boldsymbol{p}_{B,O}$ and $\boldsymbol{R}_{B,O}$. First, we figure out all feasible locations where a fixel can contact the object. Then optimal fixel locations are selected according to the criteria of localization accuracy and immobility.

3.1. Computing feasible candidate fixel locations

Problem 1. Given a formulation of the object O in $\mathscr{F}_O$, and the position $\boldsymbol{p}_{B,O}$ and orientation $\boldsymbol{R}_{B,O}$ of $\mathscr{F}_O$ w.r.t. $\mathscr{F}_{\mathrm{B}}$. Find $(\lambda_{i_1},\lambda_{i_2},\lambda_{i_3})$ such that $d(F_{\mathrm{B},i}, O_{\mathrm{B}})=0$, and compute the vector $\hat{\boldsymbol{u}}$ and the contact point $\boldsymbol{r}_{\mathrm{B},i}$.

As λ_{i_1} and λ_{i_2} are discrete and limited, we compute λ_{i_3} for every possible $(\lambda_{i_1},\lambda_{i_2})$ for which $d(F_{\mathrm{B},i}, O_{\mathrm{B}})=0$.

Step 1: Select an uninvestigated couple $(\lambda_{i_1},\lambda_{i_2})$. Set λ_{i_3} to be its lower bound. Compute $d(F_{\mathrm{B},i}, O_{\mathrm{B}})$. If $d(F_{\mathrm{B},i}, O_{\mathrm{B}})\leqslant 0$, then this location is not feasible and go to Step 4; otherwise set $\lambda_{i_3}=\lambda_{i_3}+2r_i$, where $2r_i$ is the step of search. $d(F_{\mathrm{B},i}, O_{\mathrm{B}})=0$ is also abandoned herein for lack of tolerance for manufacturing errors and adjustment.

Step 2: Compute $d(F_{\mathrm{B},i}, O_{\mathrm{B}})=0$. If $d(F_{\mathrm{B},i}, O_{\mathrm{B}})\leqslant 0$, then go to Step 3; otherwise set $\lambda_{i_3}=\lambda_{i_3}+2r_i$. If λ_{i_3} is over its upper bound, then go to Step 4; otherwise, repeat this step.

Step 3: Now there exists λ_{i_3} between $\lambda_{i_3}-2r_i$ and λ_{i_3} for which $d(F_{\mathrm{B},i}, O_{\mathrm{B}})=0$. The solution of λ_{i_3} to this equation can be found by bisection. Store $(\lambda_{i_1},\lambda_{i_2},\lambda_{i_3})$, $\hat{\boldsymbol{u}}$, and $\boldsymbol{r}_{\mathrm{B},i}$ in the feasible candidate list.

Step 4: If there exist any unchecked $(\lambda_{i_1},\lambda_{i_2})$, then return to Step 1; otherwise the procedure ends.

This procedure should be executed for the fixels of different radii and lengths on different plates, respectively.

3.2. Localization accuracy and immobilization capability

Suppose that an infinitesimal motion $\delta\boldsymbol{q}\in\mathbb{R}^6$ arises on the object, which consists of an infinitesimal translation $\delta\boldsymbol{p}\in\mathbb{R}^3$ and an infinitesimal rotation $\delta\boldsymbol{\phi}\in\mathbb{R}^3$. $\delta\boldsymbol{p}$, expressed in $\mathscr{F}_{\mathrm{B}}$, leads to the change in $\boldsymbol{p}_{B,O}$, while $\delta\boldsymbol{\varphi}$, denoting a rotation of the object about an axis through the point $\boldsymbol{p}_{B,O}$, results in the change in $\boldsymbol{R}_{B,O}$ given by

$$\delta\boldsymbol{R}=\exp(\delta\boldsymbol{\phi}^{\times}),$$

where $\delta\boldsymbol{\phi}^{\times}\in\mathbb{R}^{3\times 3}$ is the skew-symmetry matrix representing the cross product by $\delta\boldsymbol{\varphi}$. $\delta\boldsymbol{q}$ causes the movement of the object relative to the fixel at the contact point, which can be characterized by

$$\delta\boldsymbol{r}_i=\delta\boldsymbol{p}+\delta\boldsymbol{\phi}\times(\boldsymbol{r}_{\mathrm{B},i}-\boldsymbol{p}_{B,O}).$$

Let $\boldsymbol{n}_i\in\mathbb{R}^3$ denote the unit inward normal at contact i. If $\boldsymbol{n}_i^{\mathrm{T}}\delta\boldsymbol{r}_i\geqslant 0$, the object separates from fixel i. If $\boldsymbol{n}_i^{\mathrm{T}}\delta\boldsymbol{r}_i=0$, the object keeps contact with fixel i. In the two cases, $\delta\boldsymbol{q}$ is said to be consistent with fixel i. If $\boldsymbol{n}_i^{\mathrm{T}}\delta\boldsymbol{r}_i<0$, then the object collides with fixel i, and $\delta\boldsymbol{q}$ is inconsistent. Note that $\boldsymbol{n}_i^{\mathrm{T}}\delta\boldsymbol{r}_i=\boldsymbol{w}_i^{\mathrm{T}}\delta\boldsymbol{q}$ where $\boldsymbol{w}_i=\begin{bmatrix}\boldsymbol{n}_i^{\mathrm{T}} & (\boldsymbol{r}_{\mathrm{B},i}^{\mathrm{T}}-\boldsymbol{p}_{B,O}^{\mathrm{T}})\times\boldsymbol{n}_i^{\mathrm{T}}\end{bmatrix}^{\mathrm{T}}$. Let

$$\boldsymbol{G}=\begin{bmatrix}\boldsymbol{w}_1 & \boldsymbol{w}_2 & \cdots & \boldsymbol{w}_m\end{bmatrix}.$$

If $\boldsymbol{G}^{\mathrm{T}}\delta\boldsymbol{q}\geqslant 0$, then $\delta\boldsymbol{q}$ is said to be consistent.

From the definition of localization in the beginning of this paper, the object is located if and only if there does not exist nonzero $\delta\boldsymbol{q}\in\mathbb{R}^6$ satisfying $\boldsymbol{G}^{\mathrm{T}}\delta\boldsymbol{q}=\boldsymbol{0}$. This is equivalent to that the matrix $\boldsymbol{G}$ has full row rank. Following [14], we use the determinant of the matrix $\boldsymbol{M}=\boldsymbol{G}\boldsymbol{G}^{\mathrm{T}}$ as the criterion of localization accuracy, denoted by $\det\boldsymbol{M}$. A greater $\det\boldsymbol{M}$ means higher localization accuracy.

Even if an object is located, it may be still mobile. Indeed, localization only requires that six elements of $\boldsymbol{w}_1$, $\boldsymbol{w}_2,\ldots,\boldsymbol{w}_m$ are linearly independent. However, $\boldsymbol{w}_1$, $\boldsymbol{w}_2,\ldots,\boldsymbol{w}_m$ may be in the same half space, and then there exists a nonzero $\delta\boldsymbol{q}\in\mathbb{R}^6$ satisfying $\boldsymbol{G}^{\mathrm{T}}\delta\boldsymbol{q}>\boldsymbol{0}$, which implies a consistent infinitesimal motion. All consistent infinitesimal motions constitute a cone, known as the dual cone of the cone generated by $\boldsymbol{w}_1$, $\boldsymbol{w}_2,\ldots,\boldsymbol{w}_m$. An object is immobilized if and only if the dual cone contains only the origin $\boldsymbol{0}$ of $\mathbb{R}^6$ [18]. This is equivalent to that the cone generated by $\boldsymbol{w}_1$, $\boldsymbol{w}_2,\ldots,\boldsymbol{w}_m$ equals $\mathbb{R}^6$ or $\boldsymbol{0}$ lies in the interior of the convex hull of $\boldsymbol{w}_1$, $\boldsymbol{w}_2,\ldots,\boldsymbol{w}_m$. From convex analysis, the convex hull of just seven points can contain the origin $\boldsymbol{0}$ of $\mathbb{R}^6$ in its interior. On any 3-D object without rotational symmetry there always exist $\boldsymbol{w}_1$, $\boldsymbol{w}_2,\ldots,\boldsymbol{w}_7$ such that their convex hull contains $\boldsymbol{0}$ in the interior. Owing to this, we use seven fixels.

Proposition 1. *A fixture is form-closure or the object is immobilized if and only if both conditions are satisfied*:

(a) $w_1, w_2, \ldots, w_6$ *are linearly independent*,
(b) w_7 *can be written as a strictly negative combination of* $w_1, w_2, \ldots, w_6$.

Furthermore, if the conditions are satisfied, then any six of $w_1, w_2, \ldots, w_7$ *are linearly independent and the other can be uniquely written as a strictly negative combination of them.*

Referring to [18], we evaluate the capability of a fixture to immobilize an object by

$$d = -\max_{\|u\|=1}\left(\min_{i=1,2,\ldots,7} u^{\mathrm{T}} w_i\right). \tag{3}$$

In this paper, isolated d and $d(S_1, S_2)$ have different meanings. A fixture is form-closure if and only if $\min_{i=1,2,\ldots,7} u^{\mathrm{T}} w_i < 0$ for any nonzero $u \in \mathbb{R}^6$, or equivalently $d > 0$. A greater d implies superior immobilization capability. For a form-closure fixture, the convex hull of $w_1, w_2, \ldots, w_7$ is a 6-D simplex containing $\mathbf{0}$ in its interior, and d is the minimum distance from $\mathbf{0}$ to its facets. A facet of the simplex is the convex hull of six of $w_1, w_2, \ldots, w_7$. Let facet i be the convex hull of $w_{i_1}, w_{i_2}, \ldots, w_{i_6}$ where $i_1, i_2, \ldots, i_6$ are the integers between 1 and 7 other than i. The unit normal to facet i is a unit vector orthogonal to $w_{i_1} - w_{i_6}, w_{i_2} - w_{i_6}, \ldots, w_{i_5} - w_{i_6}$. Let

$$G_i = \begin{bmatrix} w_{i_1} & w_{i_2} & \cdots & w_{i_6} \end{bmatrix} \in \mathbb{R}^{6\times 6},$$

$$a = \begin{bmatrix} 1 & 1 & \cdots & 1 \end{bmatrix}^{\mathrm{T}} \in \mathbb{R}^6.$$

It can be proved that the solution of the linear system $G_i^{\mathrm{T}} u = a$ is orthogonal to $w_{i_1} - w_{i_6}, w_{i_2} - w_{i_6}, \ldots, w_{i_5} - w_{i_6}$. Since G_i is nonsingular, the unit normal can be calculated by

$$u_i = \frac{G_i^{-\mathrm{T}} a}{\left\| G_i^{-\mathrm{T}} a \right\|}, \tag{4}$$

where $G_i^{-\mathrm{T}}$ is the inverse of G_i^{T}. Moreover, u_i is outward to the simplex. Hence, the distance from $\mathbf{0}$ to the facet determined by $w_{i_1}, w_{i_2}, \ldots, w_{i_6}$ is

$$d_i = u_i^{\mathrm{T}} w_{i_1} = \left\| G_i^{-\mathrm{T}} a \right\|^{-1}. \tag{5}$$

Combining these arguments, we obtain

$$d = \min_{i=1,2,\ldots,7} d_i = \min_{i=1,2,\ldots,7} u_i^{\mathrm{T}} w_{i_1}. \tag{6}$$

3.3. Algorithms for computing optimal fixel locations

Based on the above indices two algorithms are given below.

Algorithm 1. This algorithm consists of two phases. To improve the localization accuracy, the first phase (Steps 1 and 2) is looking for the locations of 6 fixels such that $\det M$ is maximal. To achieve form-closure, the second phase (Step 3) is seeking the location of the 7th fixel such that the value of d is maximal.

Step 1: Select the initial locations at random by the computer such that $w_1, w_2, \ldots, w_6$ are linearly independent. Let $G = [\,w_1 \quad w_2 \quad \cdots \quad w_6\,]$ and $M = GG^{\mathrm{T}}$. Calculate $\det M$ and M^{-1}.

Step 2: Change the current location of a fixel to a remaining candidate to make a maximum ascent of $\det M$. If no such candidates exist for all the six fixels, then the current locations are optimal, and go to Step 3, otherwise repeat this step.

Changing the location of a fixel can be regarded as adding a fixel followed by deleting a fixel. Let M and $M_{(\pm j)}$ be the current information matrix and the one after adding or deleting the jth location, respectively. Then from [14] we have

$$M_{(\pm j)} = M \pm w_j w_j^{\mathrm{T}}, \tag{7}$$

$$M_{(\pm j)}^{-1} = M^{-1} \mp \frac{(M^{-1} w_j)(M^{-1} w_j)^{\mathrm{T}}}{1 \pm w_j^{\mathrm{T}} M^{-1} w_j}, \tag{8}$$

$$\det M_{(\pm j)} = (1 \pm w_j^{\mathrm{T}} M^{-1} w_j) \det M. \tag{9}$$

Let $M_{(+j,\,-i)}$ denote the information matrix resulting from adding the jth location followed by deleting the ith location. From (7)–(9), it follows that

$$M_{(+j,-i)} = M_{(+j)} - w_i w_i^{\mathrm{T}}, \tag{10}$$

$$M_{(+j,-i)}^{-1} = M_{(+j)}^{-1} + \frac{(M_{(+j)}^{-1} w_i)(M_{(+j)}^{-1} w_i)^{\mathrm{T}}}{1 - w_i^{\mathrm{T}} M_{(+j)}^{-1} w_i}, \tag{11}$$

$$\begin{aligned} \det M_{(+j,-i)} &= (1 - w_i^{\mathrm{T}} M_{(+j)}^{-1} w_i) \det M_{(+j)} \\ &= [(1 - w_i^{\mathrm{T}} M^{-1} w_i)(1 + w_j^{\mathrm{T}} M^{-1} w_j) \\ &\quad + (w_i^{\mathrm{T}} M^{-1} w_j)^2] \det M. \end{aligned} \tag{12}$$

The effect of a location change on the localization accuracy is assessed by the ratio h_{ij} of $\det M_{(+j,\,-i)}$ to $\det M$. From (12) we have

$$h_{ij} = (1 - w_i^{\mathrm{T}} M^{-1} w_i)(1 + w_j^{\mathrm{T}} M^{-1} w_j) + (w_i^{\mathrm{T}} M^{-1} w_j)^2. \tag{13}$$

Since G is a nonsingular matrix, we have $w_i^{\mathrm{T}} M^{-1} w_i = 1$. Then (12) and (13) can be further simplified as

$$\det M_{(+j,-i)} = (w_i^{\mathrm{T}} M^{-1} w_j)^2 \det M, \tag{14}$$

$$h_{ij} = (w_i^{\mathrm{T}} M^{-1} w_j)^2. \tag{15}$$

If $w_i^{\mathrm{T}} M^{-1} w_j = 0$, then the location change leads to the matrix G being singular. Such changes must be avoided.

Therefore, we substitute the jth candidate location for which $\left|w_i^{\mathrm{T}} M^{-1} w_j\right|$ is maximal for the current location of the ith fixel. This process is circularly repeated for every fixel until $\left|w_i^{\mathrm{T}} M^{-1} w_j\right| \leqslant 1$ for all i and j.

Step 3: Find the location of the 7th fixel among the candidates satisfying $[\boldsymbol{w}_1 \quad \boldsymbol{w}_2 \quad \cdots \quad \boldsymbol{w}_6]^{-1}\boldsymbol{w}_7 < 0$ as well as maximizing d.

The primary advantage of Algorithm 1 is the high efficiency. The recursive formulas (8), (11), (14), and (15) greatly speed up the computations of $\boldsymbol{M}^{-1}$ and $\det \boldsymbol{M}$ and the assessment of candidate locations. However, the 7th fixel is regarded only as a clamp, and its effect on localization is not considered. Also, the effect of the other fixels on immobilization is not counted. Hence we give another algorithm.

Algorithm 2. This algorithm simultaneously improves the localization accuracy and the immobilization capability.

Step 1: Select the locations of seven fixels, which achieve the form-closure property. Let $\boldsymbol{G} = [\boldsymbol{w}_1 \quad \boldsymbol{w}_2 \quad \cdots \quad \boldsymbol{w}_7]$ and $\boldsymbol{M} = \boldsymbol{G}\boldsymbol{G}^{\mathrm{T}}$. Calculate $\det \boldsymbol{M}$, $\boldsymbol{M}^{-1}$, d_i, and d.

Step 2: Change a current fixel location to a remaining candidate to increase both $\det \boldsymbol{M}$ and d as much as possible. Often the maximum increases in $\det \boldsymbol{M}$ and d cannot be obtained simultaneously. Depending upon the task, one may give priority to either one. In general, we just find a candidate location to replace the current location of a fixel such that $\det \boldsymbol{M}$ and d are both increased.

First of all, the change must ensure that the fixture is still form-closure. This can be checked by determining if the conditions in Proposition 1 are satisfied. Since the initial fixture is form-closure, from Proposition 1 we see that any six columns of $\boldsymbol{G}$ are linearly independent, which implies that $\boldsymbol{G}_i$ is nonsingular for all $i = 1,2, \ldots, 7$. Then the change of the ith fixel location to the jth candidate keeps the fixture in form-closure if and only if $\boldsymbol{G}_i^{-1}\boldsymbol{w}_j < 0$.

Besides, we do not intend to compute $\det \boldsymbol{M}$ and d for every change. Instead, we utilize an index to predict which changes might probably increase both $\det \boldsymbol{M}$ and d.

Let $\boldsymbol{M}_i = \boldsymbol{G}_i\boldsymbol{G}_i^{\mathrm{T}}$. The function of the ith fixel on locating the object can be assessed by the loss ratio of $\det \boldsymbol{M}$ caused by deleting the ith fixel. From (12), it can be expressed by

$$l_i = (\det \boldsymbol{M} - \det \boldsymbol{M}_i)/\det \boldsymbol{M} = \boldsymbol{w}_i^{\mathrm{T}}\boldsymbol{M}^{-1}\boldsymbol{w}_i. \tag{16}$$

Clearly, $l_i > 0$ for $i = 1,2, \ldots, 7$. Since $\boldsymbol{G}_i$ is nonsingular, we have $\det \boldsymbol{M}_i > 0$; thus $l_i < 1$ for $i = 1,2, \ldots, 7$. From (13) and (16), we first see that a smaller l_i may possible results in a greater h_{ij}. Moreover, l_i will be used in computing h_{ij}; thus calculating l_i does not cause any extra computation.

The function of the ith fixel on restraining the object can be evaluated by the minimum distance from $\boldsymbol{0}$ to the facets containing $\boldsymbol{w}_i$, which is formulated by

$$g_i = \min_{k=1,2,\ldots,7 \text{ and } k \neq i} d_k. \tag{17}$$

Clearly, $g_i = d$ for six of $i = 1,2, \ldots, 7$, for which $\boldsymbol{w}_i$ lies in the facet closest to $\boldsymbol{0}$, and $g_i > d$ for the other, for which $\boldsymbol{w}_i$ is not in the closest facet. Note that d_i is the smallest for the i for which $\boldsymbol{w}_i$ is not in the closest facet; thus computing g_i for $i = 1,2, \ldots, 7$ just needs to calculate g_i for the i for which d_i is the smallest, and g_i for the others is equal to d. Changing the position of the ith fixel for which $g_i > d$ cannot increase d.

Therefore, we start computing h_{ij} from i for which g_i is equal to d and l_i is relatively smaller, and continue the computation until $\det \boldsymbol{M}$ and d are both increased. Also, disregarding g_i, we may compute h_{ij} first for the i for which l_i is the smallest. By this means, a desired change can be found more quickly.

4. Measuring and adjusting

Fixtured in light of the computed fixel locations, the object may deviate a little from the desired pose in practice. Hence, in this section we discuss how to measure the location error and how to adjust the lengths of fixels to reduce it.

4.1. Measuring

We measure the actual position $\boldsymbol{p}_{B,O}$ and orientation $\boldsymbol{R}_{B,O}$ of $\mathscr{F}_O$ w.r.t. $\mathscr{F}_{\mathrm{B}}$ on a three-coordinate measuring machine (Fig. 3). To begin with, at least three marks are accurately put on the setup in order that $\mathscr{F}_{\mathrm{B}}$ can be determined from these marks. Similarly, at least three marks are attached to the object to specify $\mathscr{F}_O$. Then by detecting the coordinates of these marks, $\boldsymbol{p}_{B,O}$ and $\boldsymbol{R}_{B,O}$ can be determined.

However, the marks denoting $\mathscr{F}_O$ may be hidden after the object is clamped, so that their coordinates are not obtainable.

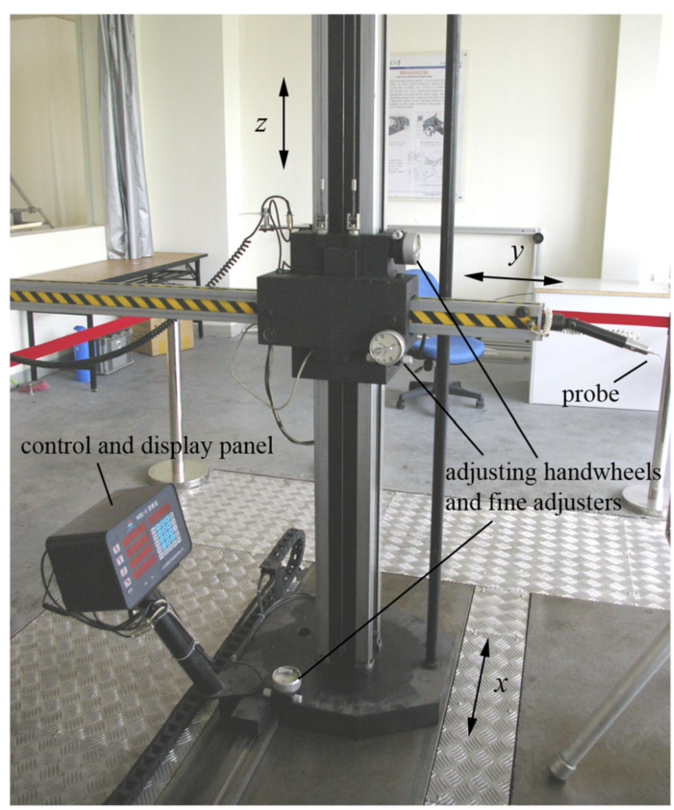

Fig. 3. Three-coordinate measuring machine.

In this case, we attach other marks to the object surface to ensure that three noncollinear marks can be detected so as to create a local coordinate frame $\mathscr{F}_C$ on the object. Denote the three marks by $\boldsymbol{c}_1$, $\boldsymbol{c}_2$ $\boldsymbol{c}_3$. By determining the coordinates of $\boldsymbol{c}_1$, $\boldsymbol{c}_2$, $\boldsymbol{c}_3$ together with those marks specifying $\mathscr{F}_O$ before the object is loaded, the coordinates of $\boldsymbol{c}_1$, $\boldsymbol{c}_2$, $\boldsymbol{c}_3$ in $\mathscr{F}_O$ can be calculated, denoted by $\boldsymbol{c}_{O,1}$, $\boldsymbol{c}_{O,2}$, $\boldsymbol{c}_{O,3}$. Then the position and orientation of $\mathscr{F}_C$ w.r.t. $\mathscr{F}_O$ can be selected as

$$\boldsymbol{p}_{O,C} = \boldsymbol{c}_{O,1}, \quad \boldsymbol{R}_{O,C} = \begin{bmatrix} \boldsymbol{x}_1 & \boldsymbol{y}_1 & \boldsymbol{x}_1 \times \boldsymbol{y}_1 \end{bmatrix}, \tag{18}$$

where

$$\boldsymbol{x}_1 = \frac{\boldsymbol{c}_{O,2} - \boldsymbol{c}_{O,1}}{\|\boldsymbol{c}_{O,2} - \boldsymbol{c}_{O,1}\|}, \quad \boldsymbol{y}_1 = \frac{(\boldsymbol{I} - \boldsymbol{x}_1\boldsymbol{x}_1^{\mathrm{T}})(\boldsymbol{c}_{O,3} - \boldsymbol{c}_{O,1})}{\|(\boldsymbol{I} - \boldsymbol{x}_1\boldsymbol{x}_1^{\mathrm{T}})(\boldsymbol{c}_{O,3} - \boldsymbol{c}_{O,1})\|}. \tag{19}$$

After the object is fixtured, we detect the coordinates of $\boldsymbol{c}_1$, $\boldsymbol{c}_2$, $\boldsymbol{c}_3$ together with the marks denoting $\mathscr{F}_B$ to determine $\boldsymbol{c}_{B,1}$, $\boldsymbol{c}_{B,2}$, $\boldsymbol{c}_{B,3}$. Then the position $\boldsymbol{p}_{B,C}$ and orientation $\boldsymbol{R}_{B,C}$ of $\mathscr{F}_C$ w.r.t. $\mathscr{F}_B$ can be readily calculated from (18) and (19) by replacing the subscript O by B. Consequently, we have

$$\boldsymbol{p}_{B,O} = \boldsymbol{c}_{B,1} - \boldsymbol{R}_{B,C}\boldsymbol{R}_{O,C}^{\mathrm{T}}\boldsymbol{c}_{O,1}, \quad \boldsymbol{R}_{B,O} = \boldsymbol{R}_{B,C}\boldsymbol{R}_{O,C}^{\mathrm{T}}. \tag{20}$$

4.2. Adjusting

Let $\boldsymbol{p}_{B,O}^*$ and $\boldsymbol{R}_{B,O}^*$ be the desired position and orientation of the object. Then the location error is given by

$$\delta\boldsymbol{p} = \boldsymbol{p}_{B,O}^* - \boldsymbol{p}_{B,O}, \quad \delta\boldsymbol{R} = \boldsymbol{R}_{B,O}^*\boldsymbol{R}_{B,O}^{\mathrm{T}}. \tag{21}$$

The matrix $\delta\boldsymbol{R} \in SO(3)$ represents a rotation about an axis $\boldsymbol{\omega} \in \mathbb{R}^3$ through an angle $\theta \in [0, 2\pi)$:

$$\theta = \cos^{-1}\left(\frac{r_{11} + r_{22} + r_{33} - 1}{2}\right), \tag{22}$$

$$\boldsymbol{\omega} = \frac{1}{2\sin\theta}\begin{bmatrix} r_{32} - r_{23} \\ r_{13} - r_{31} \\ r_{21} - r_{12} \end{bmatrix}, \tag{23}$$

where r_{ij} are the entries of $\delta\boldsymbol{R}$. The values of $\|\delta\boldsymbol{p}\|$ and θ evaluate the magnitude of the location error. If they are not small enough, we need to adjust λ_{i_3} to reduce both of them.

The required adjustment can be regarded as an infinitesimal motion of the object, which consists of $\delta\boldsymbol{p}$ and $\theta\boldsymbol{\omega}$. It will cause the movement at the contact point specified by

$$\delta\boldsymbol{r}_i = \delta\boldsymbol{p} + \theta\boldsymbol{\omega} \times (\boldsymbol{r}_{B,i} - \boldsymbol{p}_{B,O}),$$

where $\boldsymbol{r}_{B,i}$ is the ith contact position in $\mathscr{F}_B$. However, the actual value of $\boldsymbol{r}_{B,i}$ may be unobtainable. Instead we compute it w.r.t. $\boldsymbol{p}_{B,O}$, $\boldsymbol{R}_{B,O}$, and $(\lambda_{i_1}, \lambda_{i_2})$ using the method introduced in Section 3.1. Then the offense of the object against fixel i caused by the adjustment is $\delta\boldsymbol{r}_i^{\mathrm{T}}\boldsymbol{d}_{B,i}$, where $\boldsymbol{d}_{B,i}$ denotes the direction of fixel i. Therefore, the value of $\delta\boldsymbol{r}_i^{\mathrm{T}}\boldsymbol{d}_{B,i}$ can be used as a reference adjustment value of λ_{i_3}.

The procedures of measuring and adjusting probably need to be executed repeatedly for reducing the location error to an acceptable extent. Thus, the whole process of fixturing an object is summarized in Fig. 4.

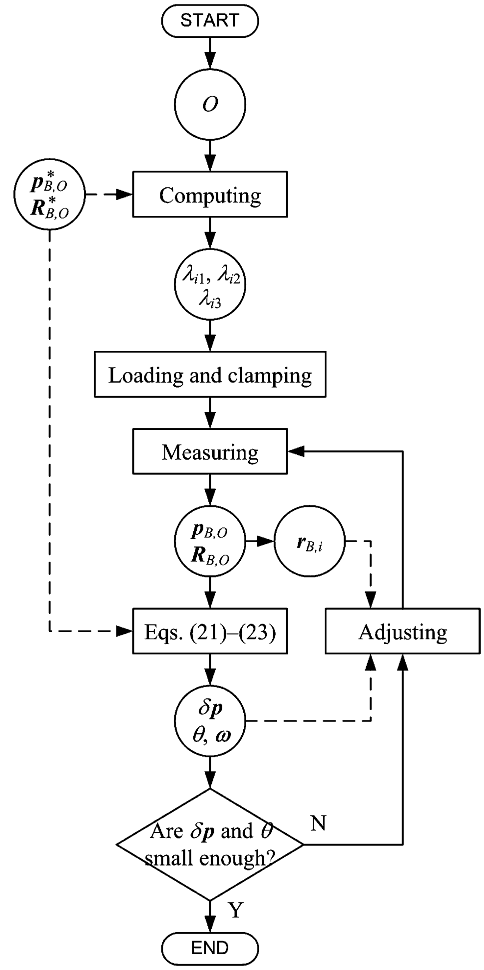

Fig. 4. Fixturing process. The solid lines indicate the principal flows, while the dashed lines indicate the auxiliary data flows. ($\boldsymbol{p}_{B,O}^*$, $\boldsymbol{R}_{B,O}^*$) and ($\boldsymbol{p}_{B,O}$, $\boldsymbol{R}_{B,O}$) give the desired and actual poses of the object, respectively.

5. Case studies

We implement the proposed algorithms using MATLAB on a Pentium-M notebook.

Example 1. The first object to be fixtured is a bottle, whose body is used for fixturing and characterized by a point cloud comprising $\boldsymbol{x}_1, \boldsymbol{x}_2, \ldots, \boldsymbol{x}_N$, where $N = 17{,}060$. Since the body is convex, we may compute $d(F_{B,i}, O_B)$ by (1) and

$$\min_{x \in O} \boldsymbol{u}^{\mathrm{T}}\boldsymbol{R}_{B,O}\boldsymbol{x} = \min \boldsymbol{u}^{\mathrm{T}}\boldsymbol{R}_{B,O}[\,\boldsymbol{x}_1 \quad \boldsymbol{x}_2 \quad \cdots \quad \boldsymbol{x}_N\,].$$

The desired object pose is selected as the following form:

$$\boldsymbol{p}_{B,O}^* = \begin{bmatrix} 0 \\ 0 \\ \alpha_1 \end{bmatrix},$$

$$\boldsymbol{R}_{B,O}^* = \begin{bmatrix} \cos\alpha_3 & -\sin\alpha_2\sin\alpha_3 & -\cos\alpha_2\sin\alpha_3 \\ 0 & \cos\alpha_2 & -\sin\alpha_2 \\ \sin\alpha_3 & \sin\alpha_2\cos\alpha_3 & \cos\alpha_2\cos\alpha_3 \end{bmatrix}. \tag{24}$$

First, we take $\alpha_1 = 70\,\text{mm}$, $\alpha_2 = \pi/2$, and $\alpha_3 = 7\pi/12$. The candidate locations for fixels are figured out by the procedure given in Section 3.1. The fixel locations are first computed by Algorithm 1 and further optimized by Algorithm 2. Then the computed fixtures are depicted in Fig. 5, where (a) shows type $\{3+2+2\}$ and (b) shows type $\{3+3+1\}$. The CPU times for computing the two fixtures are 92.18 and 98.12 s.

Second, let $\alpha_1 = 70\,\text{mm}$, $\alpha_2 = 5\pi/12$, and $\alpha_3 = 11\pi/12$. Then the optimal fixtures are shown in Fig. 5(c) and (d). The CPU times are 116.57 and 121.26 s.

Example 2. It is required to fixture a mouse, whose surface is described by 16,281 points. Its pose is also given by (24). First, set $\alpha_1 = 60\,\text{mm}$, $\alpha_2 = -\pi/3$, and $\alpha_3 = \pi/12$. Fig. 6(a) and (b) exhibit the computed fixtures of types $\{3+2+2\}$ and $\{3+3+1\}$, respectively, with the CPU times of 110.30 and 102.45 s. Second, put $\alpha_1 = 70\,\text{mm}$, $\alpha_2 = \pi/2$, and $\alpha_3 = \pi/2$. The computed fixtures are shown in Fig. 6(c) and (d). The CPU times are 76.84 and 68.80 s.

Apparently, neither the bottle nor the mouse is complex in geometry. Nevertheless, in both cases, their required poses are arbitrarily given. It is equivalent to complicating the objects. Generalizing the method herein to complex objects is straightforward.

6. Experiments

Experiment 1. First we demonstrate the repeatability of the modular fixture. It is required to show that the pose of the reloaded object is invariant as long as the fixel locations keep unchanged. Let $\boldsymbol{p}_{B,O}$ and $\boldsymbol{R}_{B,O}$ be the original position and orientation of the fixtured object and $\boldsymbol{p}'_{B,O}$ and $\boldsymbol{R}'_{B,O}$ the ones after reloading it without adjusting the fixels. Then the repeatability can be evaluated also using (21) and (22) by substituting $\boldsymbol{p}'_{B,O}$, $\boldsymbol{R}'_{B,O}$ for $\boldsymbol{p}^*_{B,O}$, $\boldsymbol{R}^*_{B,O}$. The smaller $\delta\boldsymbol{p}$ and θ mean the higher repeatability.

First, we load the bottle following Example 1, case (d). The marks are shown in Fig. 7. From their detected coordinates, the obtained coordinates of $\boldsymbol{c}_1$, $\boldsymbol{c}_2$, $\boldsymbol{c}_3$ in $\mathscr{F}_O$ and $\mathscr{F}_B$ are

$$\boldsymbol{c}_{O,1} = \begin{bmatrix} 7.0616 \\ -30.9493 \\ -14.9117 \end{bmatrix}, \quad \boldsymbol{c}_{O,2} = \begin{bmatrix} -43.9270 \\ -30.0398 \\ -15.4176 \end{bmatrix},$$

$$\boldsymbol{c}_{O,3} = \begin{bmatrix} 9.2149 \\ -31.4037 \\ 6.9338 \end{bmatrix}, \quad \boldsymbol{c}_{B,1} = \begin{bmatrix} 4.2441 \\ 3.6325 \\ 103.7941 \end{bmatrix},$$

$$\boldsymbol{c}_{B,2} = \begin{bmatrix} 53.1198 \\ 4.6830 \\ 89.9193 \end{bmatrix}, \quad \boldsymbol{c}_{B,3} = \begin{bmatrix} 0.5755 \\ -17.1700 \\ 98.1994 \end{bmatrix}.$$

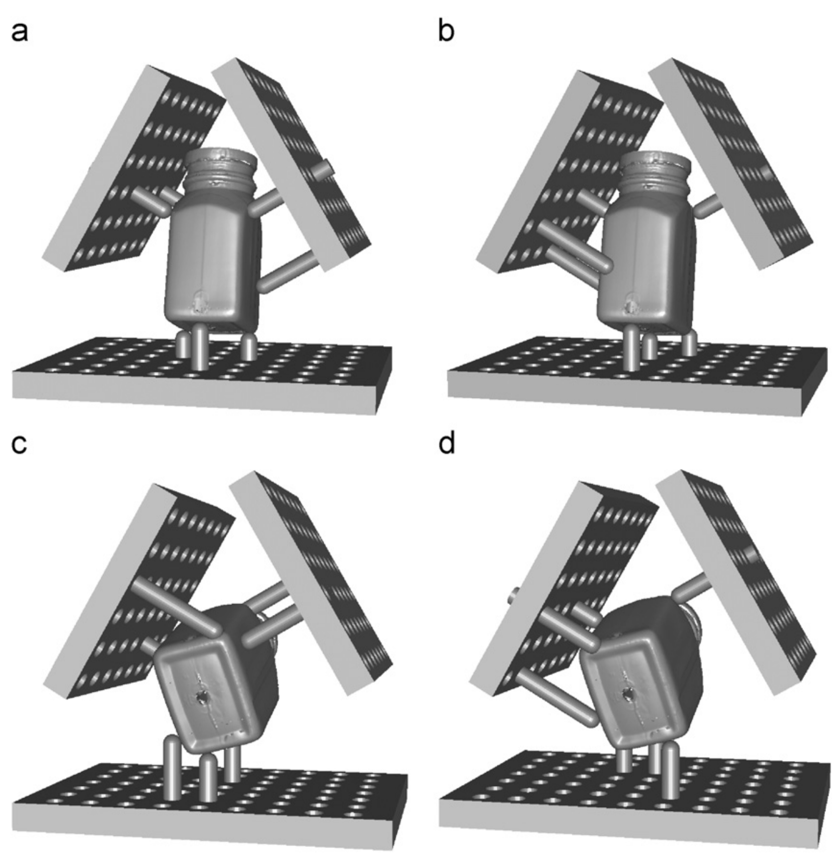

Fig. 5. Optimal locations of fixels on a bottle in two poses: (a, c) Type $\{3+2+2\}$. (b, d) Type $\{3+3+1\}$.

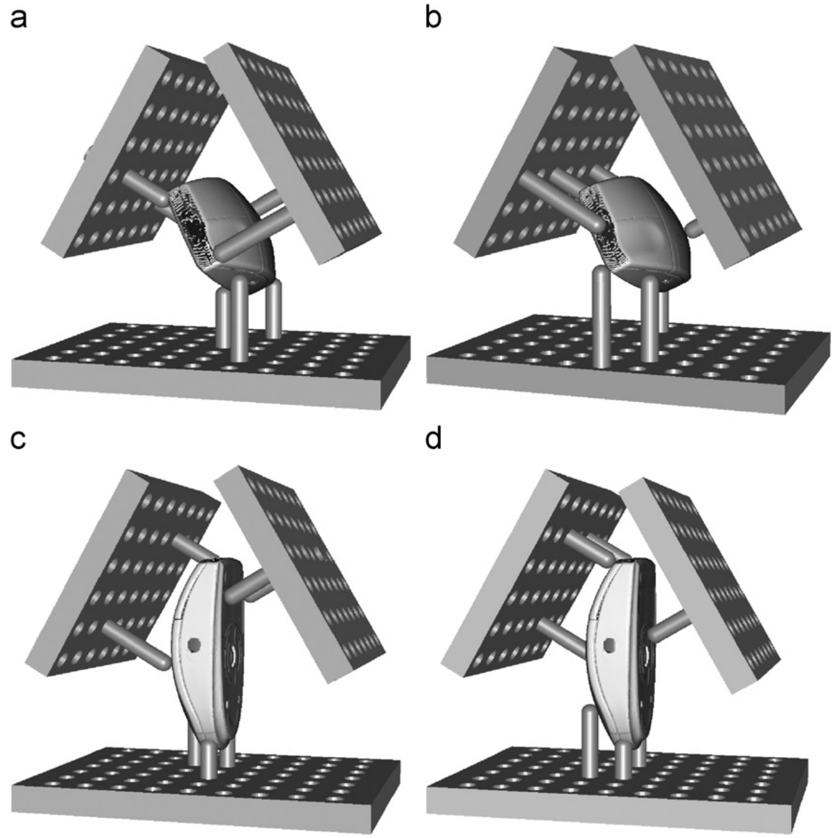

Fig. 6. Optimal locations of fixels on a mouse in two poses: (a, c) Type {3+2+2}. (b, d) Type {3+3+1}.

Then computed by (18)–(20) the pose of the bottle is

$$\boldsymbol{p}_{B,O} = \begin{bmatrix} 2.2417 \\ -0.8306 \\ 69.0643 \end{bmatrix},$$

$$\boldsymbol{R}_{B,O} = \begin{bmatrix} -0.9657 & -0.2485 & -0.0759 \\ -0.0057 & 0.3122 & -0.9500 \\ 0.2597 & -0.9169 & -0.3029 \end{bmatrix}.$$

After reloading the bottle, we have

$$\boldsymbol{c}'_{\mathrm{B},1} = \begin{bmatrix} 4.2043 \\ 3.6435 \\ 103.7741 \end{bmatrix}, \quad \boldsymbol{c}'_{\mathrm{B},2} = \begin{bmatrix} 53.0900 \\ 4.6938 \\ 89.8894 \end{bmatrix},$$

$$\boldsymbol{c}'_{\mathrm{B},3} = \begin{bmatrix} 0.5257 \\ -17.1587 \\ 98.1694 \end{bmatrix}.$$

$$\boldsymbol{p}'_{B,O} = \begin{bmatrix} 2.1961 \\ -0.8006 \\ 69.0423 \end{bmatrix}, \quad \boldsymbol{p}'_{B,O} = \begin{bmatrix} 2.1961 \\ -0.8006 \\ 69.0423 \end{bmatrix},$$

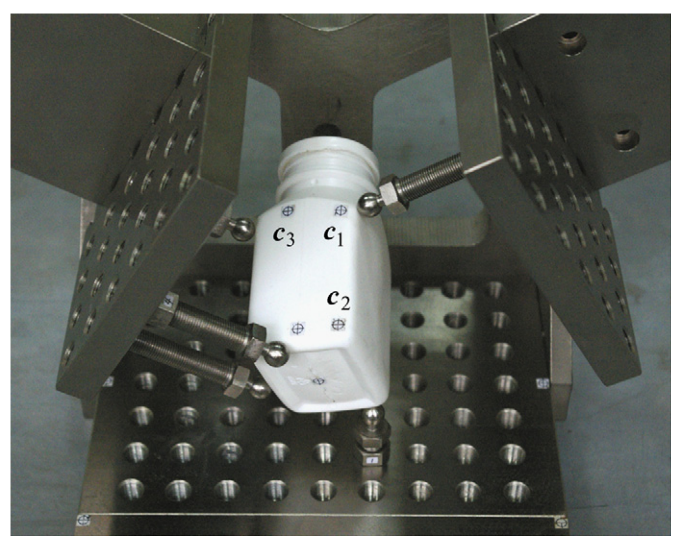

Fig. 7. A bottle fixtured on the setup.

$$\boldsymbol{R}'_{B,O} = \begin{bmatrix} -0.9656 & -0.2486 & -0.0761 \\ -0.0057 & 0.3127 & -0.9498 \\ 0.2599 & -0.9167 & -0.3034 \end{bmatrix}.$$

Then by (21) and (22), $\|\delta \boldsymbol{p}\| = 0.0458$ and $\theta = 0.0006$.

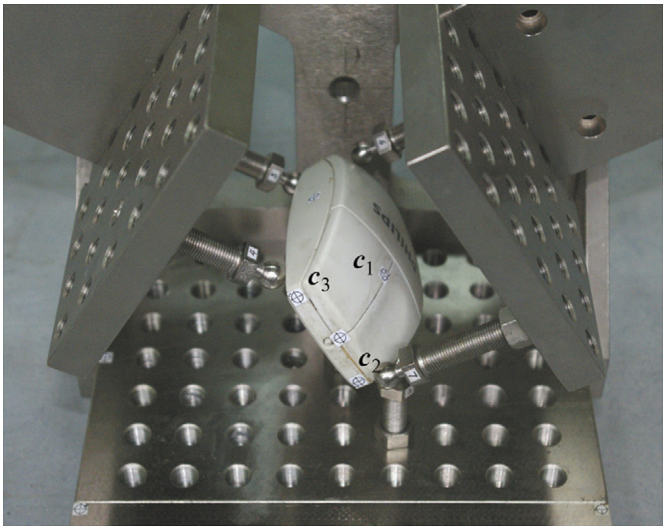

Fig. 8. A mouse fixtured on the setup.

Next, we fixture the mouse following Example 2, case (a). Fig. 8 shows the marks. The coordinates of $\boldsymbol{c}_1$, $\boldsymbol{c}_2$, $\boldsymbol{c}_3$ in $\mathscr{F}_O$ and $\mathscr{F}_B$ are

$$\boldsymbol{c}_{O,1} = \begin{bmatrix} 32.2508 \\ -1.0287 \\ 19.0724 \end{bmatrix}, \quad \boldsymbol{c}_{O,2} = \begin{bmatrix} 54.9862 \\ 20.2141 \\ -4.4450 \end{bmatrix},$$

$$\boldsymbol{c}_{O,3} = \begin{bmatrix} 54.7611 \\ -20.9877 \\ -3.7798 \end{bmatrix},$$

$$\boldsymbol{c}_{B,1} = \begin{bmatrix} 27.6888 \\ 14.6764 \\ 77.3240 \end{bmatrix}, \quad \boldsymbol{c}_{B,2} = \begin{bmatrix} 58.1268 \\ 7.3946 \\ 53.4178 \end{bmatrix},$$

$$\boldsymbol{c}_{B,3} = \begin{bmatrix} 49.1306 \\ -15.0364 \\ 86.6763 \end{bmatrix}.$$

Then computed by (18)–(20) the pose of the bottle is

$$\boldsymbol{p}_{B,O} = \begin{bmatrix} -0.1514 \\ -1.0575 \\ 57.7716 \end{bmatrix},$$

$$\boldsymbol{R}_{B,O} = \begin{bmatrix} 0.9646 & 0.2093 & -0.1602 \\ 0.0160 & 0.5603 & 0.8282 \\ 0.2631 & -0.8014 & 0.5371 \end{bmatrix}.$$

After reloading the bottle, we have

$$\boldsymbol{c}'_{B,1} = \begin{bmatrix} 27.6379 \\ 14.6381 \\ 77.3039 \end{bmatrix}, \quad \boldsymbol{c}'_{B,2} = \begin{bmatrix} 58.1056 \\ 7.3551 \\ 53.4677 \end{bmatrix},$$

$$\boldsymbol{c}'_{B,3} = \begin{bmatrix} 49.1693 \\ -15.0778 \\ 86.7061 \end{bmatrix}.$$

$$\boldsymbol{p}'_{B,O} = \begin{bmatrix} -0.2024 \\ -1.0858 \\ 57.7516 \end{bmatrix},$$

$$\boldsymbol{R}'_{B,O} = \begin{bmatrix} 0.9642 & 0.2101 & -0.1617 \\ 0.0172 & 0.5591 & 0.8289 \\ 0.2645 & -0.8020 & 0.5355 \end{bmatrix}.$$

Then by (21) and (22), $\|\delta \boldsymbol{p}\| = 0.0616$ and $\theta = 0.0024$.

In addition, we try to decrease the number of fixels to $\{3+2+1\}$ or $\{3+1+2\}$. Then both bottle and mouse fall from the fixels while being clamped. This means that six fixels are insufficient for holding a 3-D object.

When we increase the fixel number to $\{3+4+1\}$ or $\{3+3+2\}$, only seven fixels contact the object, while the other separates from the object. This implies that eight fixels overdetermine the pose of a 3-D object and the idle one is redundant.

Table 1
Adjusting the lengths of fixels for reducing the location error on the bottle

i	1	2	3	4	5	6	7	$\|\delta \boldsymbol{p}\|$	θ
λ_{i_3}	26.00	35.21	45.35	50.53	33.39	66.50	49.40	2.5672	0.0560
Δ_1	−0.06	0.80	1.52	0.70	0.25	−1.25	0	1.5349	0.0402
Δ_2	0.40	−0.50	−0.30	1.05	0.50	0.20	0	0.8250	0.0280
Δ_3	0.70	−0.50	−0.45	1.20	0.35	0.85	0	0.2895	0.0148

Table 2
Adjusting the lengths of fixels for reducing the location error on the mouse

i	1	2	3	4	5	6	7	$\|\delta \boldsymbol{p}\|$	θ
λ_{i_3}	30.49	42.36	31.76	43.89	59.06	53.27	53.66	2.4712	0.0731
Δ_1	1.50	0.85	1.25	−0.20	0.60	−3.80	0.20	1.1131	0.0598
Δ_2	1.00	0.15	0.40	0	0.85	−3.50	0.70	0.8278	0.0352
Δ_3	0.50	0.30	−0.15	0.60	−0.75	−0.05	0	0.2251	0.0168

Experiment 2. We need to demonstrate the effectiveness of the adjusting method. First, the bottle and mouse are fixtured initially as in Experiment 1. Tables 1 and 2 list the adjustments together with the variation of $\|\delta \boldsymbol{p}\|$ and θ. It can be seen that by adjusting the location errors are greatly reduced. Figs. 7 and 8 show their final poses.

7. Conclusions

This paper investigates 3-D modular fixtures in a systematic way. First, by repeated reviewing and improving, a 3-D modular fixture emerges, particularly aiming to fixture 3-D complex objects or locate objects in arbitrary poses. Then, a mathematical model of the fixture is established. On this basis, we develop algorithms for automatically selecting the optimal fixel locations on the baseplates to precisely locate and firmly clamp the object. Later, methods for measuring the location error and for adjusting the fixels to improve the localization accuracy are presented. Finally, all the work is illustrated by case studies with experiments.

Although this paper focuses on a typical 3-D modular fixture, such complete experience of developing this important tool from principles to practice is a useful reference for manufacturers.

Acknowledgments

This work was supported by the National Natural Science Foundation of China under Grant 59685004. The authors are very grateful to the editors and the reviewers for their careful review.

Appendix. A distance function of sets

Let S_1 and S_2 be compact sets with nonempty interiors in $\mathbb{R}^l$. The distance function of S_1 and S_2 is defined by

$$d(S_1, S_2) = \begin{cases} \min\limits_{\lambda B_0 \cap (S_1 - S_2) \neq \emptyset, \lambda \geqslant 0} \lambda & \text{if } S_1 \cap S_2 = \emptyset, \\ \min\limits_{\lambda B_0 \subset S_1 - S_2, \lambda \leqslant 0} \lambda & \text{if } S_1 \cap S_2 \neq \emptyset, \end{cases}$$

where $S_1 - S_2 = \{\boldsymbol{x}_1 - \boldsymbol{x}_2 \in \mathbb{R}^l | \boldsymbol{x}_1 \in S_1,\ \boldsymbol{x}_2 \in S_2\}$ and $B_0 = \{\boldsymbol{u} \in \mathbb{R}^l | \boldsymbol{u}^{\mathrm{T}}\boldsymbol{u} = 1\}$. If $S_1 \cap S_2 = \emptyset$, then $d(S_1,\ S_2)$ is positive and equal to the distance between the closest points in S_1 and S_2. If $\mathrm{int}S_1 \cap \mathrm{int}S_2 \neq \emptyset$ where $\mathrm{int}(\cdot)$ denotes the interior of a set, then $d(S_1,\ S_2)$ is negative and equal to the minimum translation to separate S_1 and S_2. Otherwise, $d(S_1,\ S_2) = 0$, and S_1 just contacts S_2 at the boundaries.

If S_1 and S_2 are convex, then the distance function can be rewritten in a unified form as

$$\begin{aligned} d(S_1, S_2) &= -\min_{\|\boldsymbol{u}\|=1} \left(\max_{\boldsymbol{x}_1 \in S_1,\ \boldsymbol{x}_2 \in S_2} \boldsymbol{u}^{\mathrm{T}}(\boldsymbol{x}_1 - \boldsymbol{x}_2) \right) \\ &= -\min_{\|\boldsymbol{u}\|=1} \left(\max_{\boldsymbol{x}_1 \in S_1} \boldsymbol{u}^{\mathrm{T}}\boldsymbol{x}_1 - \min_{\boldsymbol{x}_2 \in S_2} \boldsymbol{u}^{\mathrm{T}}\boldsymbol{x}_2 \right). \end{aligned}$$

For detailed derivation of the above equation, one may refer to [19]. Furthermore, suppose that $\hat{\boldsymbol{u}}$ is the vector such that $d(S_1, S_2) = -\max_{\boldsymbol{x}_1 \in S_1} \hat{\boldsymbol{u}}^{\mathrm{T}}\boldsymbol{x}_1 + \min_{\boldsymbol{x}_2 \in S_2} \hat{\boldsymbol{u}}^{\mathrm{T}}\boldsymbol{x}_2$. Let $\hat{S}_1$ (resp. $\hat{S}_2$) be the set of $\hat{\boldsymbol{x}}_1 \in S_1$ (resp. $\hat{\boldsymbol{x}}_2 \in S_2$) such that $\max_{\boldsymbol{x}_1 \in S_1} \hat{\boldsymbol{u}}^{\mathrm{T}}\boldsymbol{x}_1 = \hat{\boldsymbol{u}}^{\mathrm{T}}\hat{\boldsymbol{x}}_1$ (resp. $\min_{\boldsymbol{x}_2 \in S_2} \hat{\boldsymbol{u}}^{\mathrm{T}}\boldsymbol{x}_2 = \hat{\boldsymbol{u}}^{\mathrm{T}}\hat{\boldsymbol{x}}_2$). If $d(S_1,\ S_2) = 0$, then $S_1 \cap S_2$ equals $\hat{S}_1 \cap \hat{S}_2$, and $\hat{\boldsymbol{u}}$ is the normal at contact outward to S_1 and inward to S_2.

References

[1] A.Y.C. Nee, Z.J. Tao, A.S. Kumar, An advanced Treatise on Fixture Design and Planning, World Scientific, London, 2004.
[2] R.C. Brost, K.Y. Goldberg, A complete algorithm for designing planar fixtures using modular components, IEEE Transactions on Robotics and Automation 12 (1) (1996) 31–46.
[3] A.S. Wallack, J.F. Canny, Planning for modular and hybrid fixtures, Algorithmica 19 (1) (1997) 40–60.
[4] A.S. Wallack, Generic fixture design algorithm for minimal modular fixture toolkits, in: Proceedings of the IEEE International Conference on Robotics and Automation, Minneapolis, MN, April 1996, pp. 487–494.
[5] Y. Wu, Y. Rong, W. Ma, S.R. LeClair, Automated modular fixture planning: geometric analysis, Robotics and Computer-Integrated Manufacturing 14 (1) (1998) 1–15.
[6] Y. Wu, Y. Rong, W. Ma, S.R. LeClair, Automated modular fixture planning: accuracy clamping and accessibility analyses, Robotics and Computer-Integrated Manufacturing 14 (1) (1998) 17–26.
[7] D.T. Pham, A.D.S. Lazaro, AutoFix—an expert CAD system for jigs and fixtures, International Journal of Machine Tools and Manufacturing 30 (3) (1990) 403–411.
[8] J.R. Dai, A.Y.C. Nee, J.Y.H. Fuh, A.S. Kumar, An approach to automating modular fixture design and assembly, Proceedings of the Institution of Mechanical Engineers: Part B, Journal of Engineering Manufacture 211 (B7) (1997) 509–521.
[9] A.S. Kumar, A.Y.C. Nee, S. Prombanpong, Expert fixture-design system for an automated manufacturing environment, Computer-Aided Design 24 (4) (1992) 316–326.
[10] A.S. Kumar, J.Y.H. Fuh, T.S. Kow, An automated design and assembly of interference-free modular fixture setup, Computer-Aided Design 32 (10) (2000) 583–596.
[11] J.L. Hou, A.J.C. Trappey, Computer-aided fixture design system for comprehensive modular fixtures, International Journal of Production Research 39 (16) (2001) 3703–3725.
[12] W.-H. Qian, H. Qiao, An efficient algorithm for computing object poses in a modular fixture or gripper, Journal of Robotic Systems 19 (3) (2002) 99–114.
[13] F. Mervyn, A.S. Kumar, A.Y.C. Nee, Automated synthesis of modular fixture designs using an evolutionary search algorithm, International Journal of Production Research 43 (23) (2005) 5047–5070.
[14] M.Y. Wang, D.M. Pelinescu, Optimizing fixture layout in a point-set domain, IEEE Transactions on Robotics and Automation 17 (3) (2001) 312–323.
[15] Y. Wang, X. Chen, Q. Liu, N. Gindy, Optimisation of machining fixture layout under multi-constraints, International Journal of Machine Tools and Manufacture 46 (12–13) (2006) 1291–1300.
[16] R.G. Brown, R.C. Brost, A 3-D modular gripper design tool, IEEE Transactions on Robotics and Automation 15 (1) (1999) 174–186.
[17] W.-H. Qian, H. Qiao, S.K. Tso, Synthesizing two-fingered grippers for positioning and identifying objects, IEEE Transactions on Systems, Man, and Cybernetics—Part B: Cybernetics 31 (4) (2001) 602–615.
[18] Y. Zheng, W.-H. Qian, Coping with the grasping uncertainties in force-closure analysis, International Journal of Robotics Research 24 (4) (2005) 311–327.
[19] C.E. Buckley, A foundation for the flexible-trajectory approach to numeric path planning, International Journal of Robotics Research 8 (3) (1989) 44–64.